International Society for Rock Mechanics and Rock Engineering
Norwegian Group for Rock Mechanics

ISRM International Symposium
Eurock 2025 – Expanding the Underground Space
Trondheim, Norway, 16-20 June
ISBN 978-82-8208-079-8

A simplified analytical method for bolt reinforcement of the tunnel face in deep conditions

W. Mohamad, A. Saitta & G. Rousselot
Egis Structures et Environnement – Pôle Tunnels & Ouvrages Souterrains, Annecy, France
wassim.mohamad@egis-group.com (email of corresponding author)

M. Janutolo Barlet & B. Lecomte
Vinci Construction Grands Projets, Saint-Martin de la Porte, France

Abstract

This study introduces a tunnel face bolt reinforcement technique for deep rock tunnels, based on the quantification of the plastic rock mass volume ahead of the tunnel face using the convergence-confinement method. A closed-form solution is derived for scenarios involving homogeneous ground with uniform face reinforcement. The methodology incorporates the reinforcement scheme and evaluates stability under the most critical conditions. The procedure outlines the minimum bolt length requirements and the required bolt density at the tunnel face.

A case study is conducted on the TELT (Tunnel EURALPIN LYON TURIN) project, examining stability challenges and reinforcement needs for the SMP4 segment, now part of the CO7 operational construction site in Saint-Martin-La-Porte. In this context, a tunnel was excavated in squeezing ground, including a fault zone, at an approximate depth of 550 m.

Keywords

Bolt reinforcement, tunnel face stability, analytical method

1 Introduction

Tunnel face stability is a fundamental aspect in the design and construction of underground structures. Ensuring the stability of the tunnel face is crucial to prevent collapses and ensure the safety of workers and equipment, particularly in poor ground conditions subjected to high overload. In such scenarios, the ground experiences significant inelastic straining, resulting in substantial tunnel face deformations (Lunardi 2008).

One of the most effective methods to enhance tunnel face stability in conventional tunnel excavations is through face reinforcement techniques, specifically the installation of fiberglass bolts. Various closed-form solutions for face reinforcement have been established for shallow tunnels, considering a failure mechanism involving a wedge at the face and an overlying prism extending to the soil surface (Anagnostou et Perazzelli 2015). However, these methods exhibit limited accuracy and applicability in deep tunnels due to the differing failure mechanisms (Georgiou et al. 2021).

This paper presents an analytical method for face reinforcement in deep tunnels, based on the assessment of the unstable rock mass volume ahead of the tunnel face. The analysis is conducted under the assumption of a homogeneous isotropic ground, without considering groundwater effects. The failure mechanism is governed by the development of the plastic zone around the tunnel face, which is investigated using the convergence-confinement method with the Mohr-Coulomb failure criteria.

The proposed method is applied to a case study on the TELT (Tunnel EURALPIN LYON TURIN) project. In this context, a tunnel was excavated in a squeezing rock mass, including a fault zone, at an approximate depth of 550 m. Monitoring results, including extrusions and encountered face instabilities, are provided, and face reinforcements are verified for different project sectors.

2 Tunnel face reinforcement method

2.1 Failure mechanism for shallow and deep tunnels

In conventional tunnel excavations, reinforcement of the tunnel face is typically achieved using fiberglass dowels. These reinforcement elements limit tunnel face deformation due to their passive behaviour, as they are anchored ahead of the tunnel face. The density of bolt reinforcement is usually determined to counterbalance the equivalent pressure required to ensure rock mass stability at the tunnel face. For shallow tunnels, this pressure is established using the limit equilibrium approach, which considers a complete cave-in of the ground up to the surface level (Fig. 1a). The three-dimensional visualization of the static system (Fig. 1b) includes the wedge-prism failure body, where the prismatic body exerts a load upon the wedge (Anagnostou et Kovári 1994). Failure occurs if the applied load exceeds the bearing capacity of the wedge (Anagnostou et Perazzelli 2015). The load representing the prism is calculated based on Terzaghi's silo theory. This method is commonly used for shallow tunnels in soft grounds. However, in very deep tunnels, Terzaghi's vertical stress is generally negative, resulting in a stable prism and wedge without any support pressure, even in weathered rock masses or fault zones.

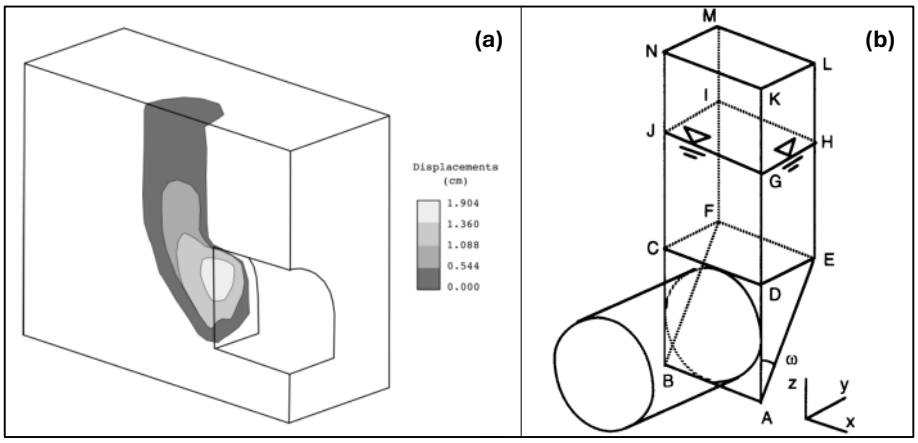

Fig. 1 (a) A 3D numerical example of the deformed grid at collapse in a case of a shallow tunnel (Fernández, et al. 2021) (b) Tunnel face failure mechanism of a shallow tunnel (Anagnostou et Kovári 1994)

In very deep rock masses, the failure mechanism of the tunnel face is a multifaceted process influenced by various factors such as in-situ stress conditions, rock mass properties, and tunnel geometry. Primarily, stress-induced failures such as spalling and rock bursting are common, where tensile stresses exceed the rock's tensile strength, causing slab formation or violent ejection of rock fragments. Shear failure mechanisms, including slabbing and wedge failure, occur along pre-existing weaknesses or newly formed fractures, resulting in the detachment of rock slabs or the dislodging of rock blocks. Additionally, squeezing ground presents a significant challenge due to the time-dependent plastic deformation of the rock mass under high in-situ stresses. This phenomenon occurs when the stress on the tunnel walls exceeds the rock mass's strength, causing the rock to deform plastically and gradually converge into the tunnel.

In the case of homogeneous rock mass behaviour without significant discontinuities or anisotropies, the deformation pattern can be characterized by a symmetric, dome-like inward bulging of the tunnel face. This failure morphology typically arises in environments where isotropic stress conditions prevail, resulting in relatively uniform in-situ stresses in all directions. Fig. 2a presents borehole recordings at the tunnel face in a shale-dominated fault zone of an SMP4 segment (Mathieu, et al. 2023), highlighting the penetration rate up to 10 meters ahead of the tunnel face. An unstable volume, referred to as "dead ground", can be observed in the form of a spherical cap. This volume can be correlated to the form and size of the plastic zone developing ahead of the tunnel face in deep isotropic rock masses (Fig. 2b).

A preliminary evaluation of the development of this plastic zone can be conducted using the concept of the stability number N, which was first introduced by (Broms et Bennemark 1967) to assess the short-term stability of the tunnel face in undrained clayey ground. However, this concept was later extended by the following expression (Panet et Sulem 2021). The plastic zone develops ahead of the tunnel face when N > 5. The face is considered stable when N <= 5.

$$\mathrm{N} = \frac{2P_0}{\sigma_{cm}} = \frac{2\gamma(H + r_0)}{\sigma_{cm}} \tag{2}$$

$$\sigma_{cm} = 2\mathrm{c}\frac{cos\phi}{1 - sin\phi} \tag{3}$$

Where P_0 In-situ stress
σ_{cm} Rock mass strength
r_0 Radius of the excavated section
γ Rock mass unit weight
c, ϕ Rock mass cohesion and friction angle
H Cover depth

Based on this evaluation, the proposed face reinforcement approach will, in a simplified manner, consider the entire plastic zone ahead of the tunnel face as the failure rock mass volume. The driving force to be supported by the face reinforcement correspond to the total weight of the plastic volume.

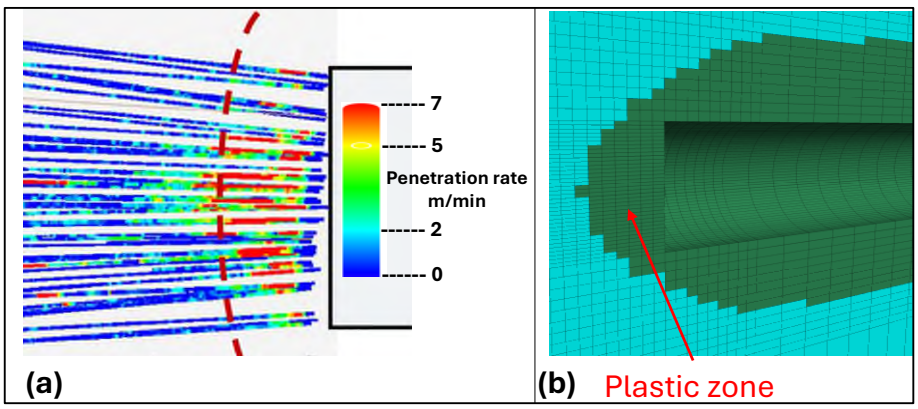

Fig. 2 (a) Unstable rock mass volume identified through borehole recordings in a Shale-dominated fault zone of an SMP4 segment (Mathieu, et al. 2023) (b) Plastic zone around a deep tunnel using a 3D numerical model

2.2 Analytical formulation of the proposed method

The self-weight F_{vp} of the plastic volume ahead of the tunnel is the sole driving force to be considered in the calculation of the face reinforcement. For simplification purposes, the plastic volume ahead of the tunnel face V_{p0} is assumed to be a spherical cap with a base radius equivalent to the radial plastic radius at tunnel face r_{p0} and a height h (Fig. 3a). The latter corresponds to the horizontal extent of the plastic zone ahead of the tunnel face. It ranges between 50 and 75 % of the plastic radius at tunnel face (Cantieni et al., 2011). We will consider the maximum ratio in this article, i.e. $h = 0.75r_{p0}$. Therefore, the corresponding self-weight F_{vp} can be estimated using to the following equation. The plastic radius at tunnel face is determined using the convergence-confinement method.

$$F_{vp} = \gamma V_{p0} = \gamma \frac{1}{6}\pi h\left(3{r_{p0}}^2 + h^2\right) = \frac{57}{128}\gamma\pi {r_{p0}}^3 \tag{4}$$

The supporting force of a single bolt is determined based on several factors, including the material properties of the bolt, the quality of the surrounding rock, the length and diameter of the bolt and the installation pattern. The bolts are typically inserted into boreholes and then anchored in place using grout or mechanical means. The calculation typically involves determining the bolt's tensile strength, the bond strength at the bolt-grout interface and the bond strength between the grout and the surrounding rock. The design of face reinforcement should be conducted considering the most critical bolt layout. The set of bolts with an initial length L is generally installed at regular intervals l (installation interval), resulting in an effective bolt length L' at the tunnel face that varies with each excavation step. The most unfavourable effective length to be considered in the calculation is L' = L-l.

Fig. 3b illustrates a simplified load transfer curve for a single bolt installed at the tunnel face. The bolt accommodates its load along a distance d_{pl} before transferring it to the rock mass over the anchoring length L_a. The anchoring length and the load accommodating distance vary over the height of the tunnel face depending on the extent of the plastic zone in the vicinity of each bolt. For computational simplicity, a uniform distance d_{pl} is considered, derived from the equivalent cylindrical volume of the plastic zone. The volume of this cylinder is given by $d_{pl}(\pi r_{p0}^2)$, leading to a distance d_{pl} that can be expressed according to Eq. 5. The initial bolt length L and the installation interval l should be selected to ensure a minimal effective length that satisfies the condition $L' > 57\ r_{p0}/128$.

$$d_{pl} = \frac{V_{p0}}{\pi {r_{p0}}^2} = \frac{\frac{57}{128}\pi {r_{p0}}^3}{\pi {r_{p0}}^2} = \frac{57}{128} r_{p0} \tag{5}$$

Based on the previous assumptions, the supporting force of each bolt (modified from (Anagnostou et Perazzelli 2015)) reads as follows:

$$F_b = \min\left[F_t, \pi d_{pl} \min\left(d\tau_m, d_b\tau_g\right), \pi L_a min\left(d\tau_m, d_b\tau_g\right)\right] \tag{6}$$

Where F_t Bolt tensile strength
d, d_b Borehole and bolt diameter, respectively
τ_m Shear strength of the grout-rock interface, assumed constant along the entire bolt
τ_g Shear strength of the grout-bolt interface, assumed constant along the entire bolt
L_a Anchoring length of the bolt = L' - d_{pl}

Eq. 6 accounts for the tensile failure of the bolt as well as the shear failure at the various interfaces both within and outside the plastic zone. The number of bolts n required to ensure tunnel face stability is determined by dividing the total weight of the plastic zone F_{vp} by the supporting force of a single bolt F_b, so that $n = F_{vp} / F_b$. The required bolt density is given by $n/\pi r_0^2$.

3 Determination of the plastic radius at tunnel face

The plastic radius is analysed through the application of the convergence-confinement method, employing the Mohr-Coulomb failure criterion as specified below:

$$\sigma_1 = \sigma_{cm} + k\sigma_3 \tag{7}$$

Where σ_1, σ_3 Maximum and minimum principal stress, respectively

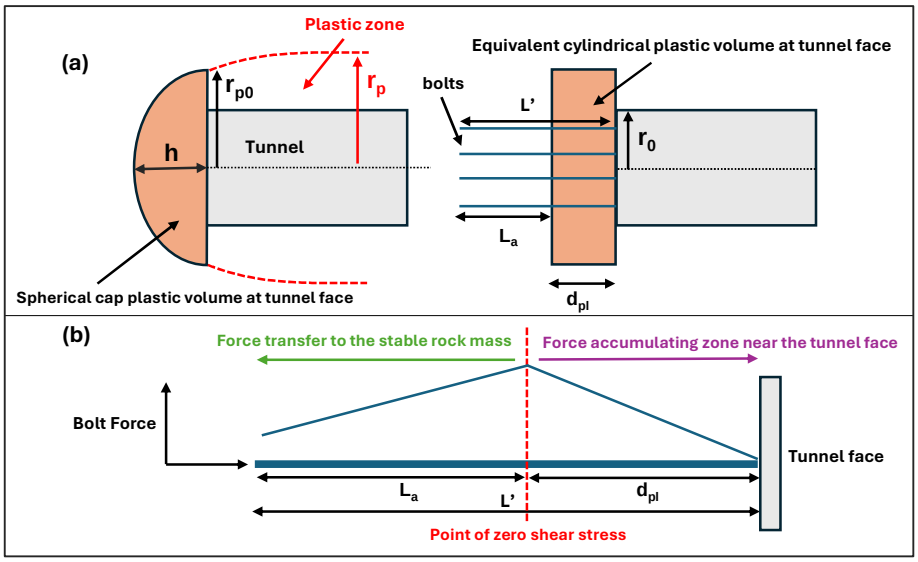

Fig. 3 (a) Unstable rock mass volume at tunnel face (b) Simplified load transfer curve for a single bolt

The slope k of the σ_1 - σ_3 curve is defined by:

$$k = \frac{1 + sin\phi}{1 - sin\phi} \tag{8}$$

We consider a circular tunnel of radius r_0 subjected to a hydrostatic stress field P_0 and a fictive support pressure P_i as illustrated in Fig. 4. Failure of the rock mass occurs when the fictive pressure P_i falls below a critical pressure P_{cr} defined as follows (Hoek 2023):

$$P_{cr} = \frac{2P_0 - \sigma_{cm}}{1 + k} \tag{9}$$

The behaviour of the rock mass is elastic when the fictive pressure is greater than the critical pressure ($P_i > P_{cr}$). In this case, the radial displacement u_i is given by:

$$u_{ie} = \frac{r_0(1 + \nu)}{E}(P_0 - P_i) \tag{10}$$

Where E, ν Rock mass Young modulus and Poisson ratio, respectively.

When failure occurs ($P_i < P_{cr}$), the plastic zone starts to develop around the circular tunnel with a corresponding plastic radius r_p that expresses as follows:

$$r_p = r_0 \left[\frac{2(P_0(k-1) + \sigma_{cm})}{(1+k)((k-1)P_i + \sigma_{cm})} \right]^{\frac{1}{k-1}} \tag{11}$$

The radial displacement in the plastic zone is given by:

$$u_{ip} = \frac{r_0(1+\nu)}{E} \left[2(1-\nu)(P_0 - P_{cr}) \left(\frac{r_p}{r_0} \right)^2 - (1-2\nu)(P_0 - P_i) \right] \tag{12}$$

The plastic radius at tunnel face is correlated to the radial displacement at tunnel face. Considering the longitudinal displacement profile develepped by (Vlachopoulos et Diederichs 2009), the radial displacement at tunnel face u_0 is determined by the following equation :

$$u_0 = \frac{u_m}{3} e^{-0.15(r_{pm}/r_0)} \tag{13}$$

Where r_{pm} Maximum plastic radius, calculated by Eq. 11 for $P_i = 0$
u_m Maximum radial displacement, calculated by Eq. 12 for $P_i = 0$

The calculated radial displacement at tunnel face u_0 allows for the determination of the corresponding fictive pressure using Eq. 12. This pressure can then be used to determine the plastic radius at tunnel

face r_{p0} using Eq. 11. To simplify the calculation, a direct relationship between r_{p0} and u_0 is given below (deduced through a series of calculations for different geomechanical rock mass properties):

$$\frac{r_{p0}}{r_{pm}} = 1.24\left(\frac{u_0}{u_m}\right)^{0.59} \tag{14}$$

The determination of the plastic radius using Eq. 14 is applicable when the stability number $N > 5$. If the equation gives $r_{p0} < r_0$, we consider $r_{p0} = r_0$. In such cases, the face reinforcement is considered "contingent," meaning it is installed only if required due to excavation difficulties.

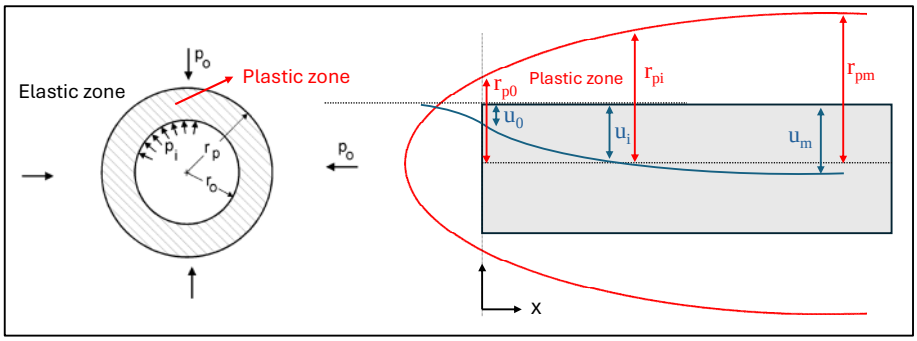

Fig. 4 Convergence-confinement method (modified from (Hoek 2023))

4 Saint-Martin-La-Porte case study

The Lyon-Turin railway project involves constructing a 67 km line linking Saint-Jean-de-Maurienne (France) to Susa (Italy), including a 57 km twin-tunnel called the Mont Cenis Base Tunnel. An exploratory tunnel (SMP4-3B) was built using conventional methods along the southern tube axis (Fig. 5) of the base tunnel (Janin, et al. 2022), to study rock mass behaviour and construction feasibility. The sector comprises sandstones and carbonaceous shale with a 550 m tunnel cover.

The support system has two phases (Fig. 5b): Phase A (top heading excavation) includes eventual Forepoling, face bolting, shotcrete, radial bolting and sliding ribs. Phase B (benching down excavation) comprises a thicker shotcrete layer and yielding blocks. Monitoring included face extrusions and radial convergences, with observed deformations between 0.5% and 10%. A back-analysis was performed to assess the rock mass properties along the southern tube. The short-term Mohr-Coulomb characteristics are presented in Table 1. Two classes (4 and 6) are excluded from the analysis as they are not represented within this sector of the project.

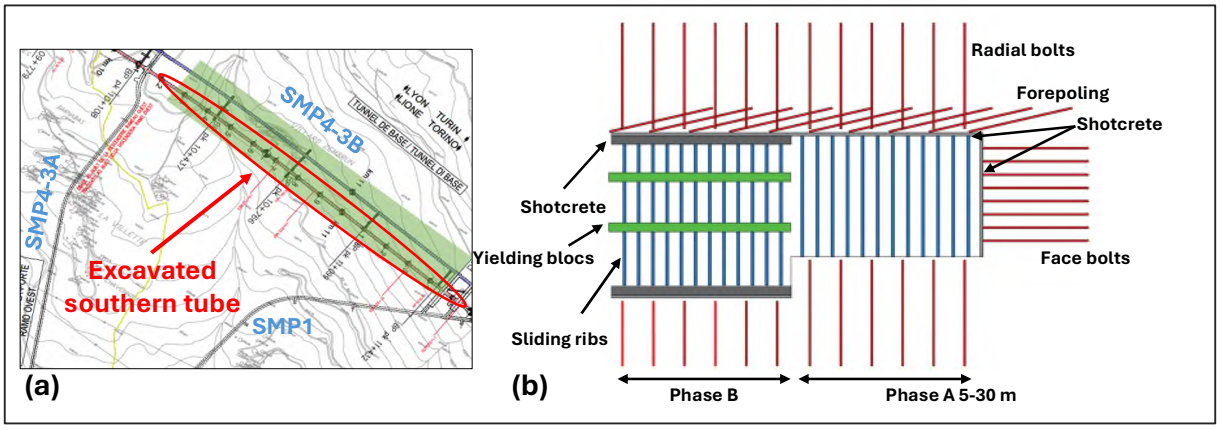

Fig. 5 (a) Saint-Martin-La-Porte work layout (b) SMP4-3B systematic support system

Table 1 Short-term characteristics of the southern tube (excluding class 4 and 6)

	Colour code	Young modulus E (MPa)	Cohesion c (MPa)	Friction angle ϕ
Class 0		7600	2	37
Class 1		2530	1.63	32.2
Class 2		1760	1.06	31.7
Class 3		1530	0.82	30
Class 5		1100	0.42	24.5

4.1 Extrusions and tunnel face instabilities

The target excavated section "large section" has a tunnel radius ranging from 6 to 6.5 m. However, under extremely squeezing conditions, initial excavation necessitated a reduced section (R = 4.4 m) or a small section (R = 3.15 m) in fault zones. Extrusions along the southern tube varied between 0.2% and nearly 10%, as illustrated in Fig. 6. Face reinforcement comprised 30 fiberglass dowels (L = 12 m, diameter = 28 mm, tensile strength = 380 kN) installed every 4-6 m in the red fault zone (class 5) with a small section, and 50 bolts installed every 2-6 m in other zones with a large section. This reinforcement pattern proved sufficient for classes 0 to 2 and largely effective for class 5. However, tunnel instability was observed in class 3 sections (collapse of the tunnel face), and shotcrete cracks (a single incident at chainage 10655 m) were noted in the fault zone. Consequently, additional face bolts (up to 20) were installed, particularly between chainage 10950 and 11200 m in the class 3 zone.

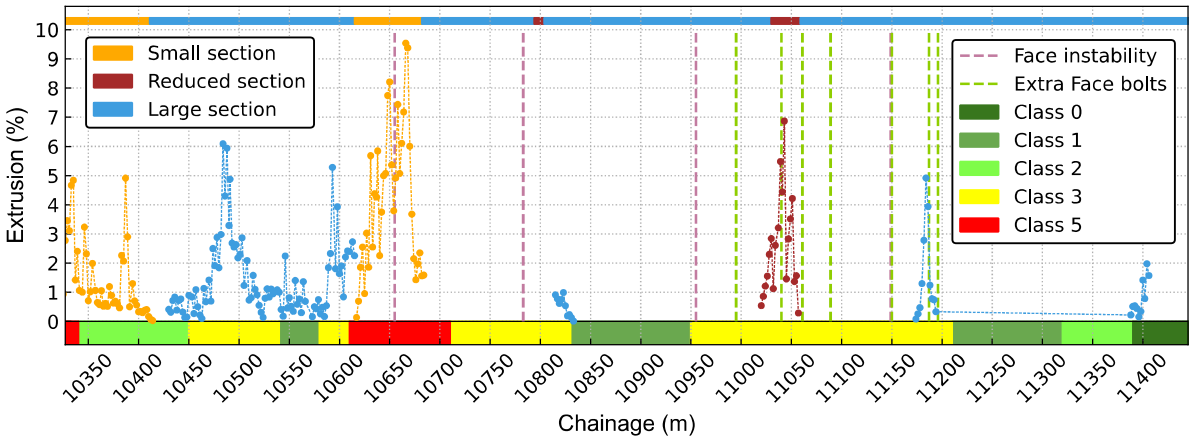

Fig. 6 Extrusions and tunnel face instabilities along the southern tube

4.2 Reinforcement verification using the proposed approach

The required bolt density will be studied for selected zones using the new simplified approach. The rock mass unit weight γ = 27 kN/m^3 and Poisson's ration ν = 0.3. The calculation is performed under the assumption of a full-face excavation. The resulting density will be used to determine the number of bolts required exclusively for the top heading. The procedure involves the following steps:

- Stability number N. If N > 5, the face is considered unstable.
- Maximum plastic radius and radial displacement using Eq. 11 and 12 for $P_i = 0$, respectively,
- Tunnel face displacement using Eq. 13 and tunnel face plastic radius using Eq.14,
- Plastic volume total weight using Eq. 4.
- Supporting force of each bolt using Eq. 6, we consider a more critical shear failure possibility at grout-bolt interface with a shear stress of 1 MPa.
- Bolt density = $n/\pi r_0^2 = (F_{vp} / F_b)/ \pi r_0^2$.
- Number of bolts for the top heading: (bolt density) x (excavated section of the top heading).

For a rock mass of Class 2, the required number of bolts was determined to be 34 (50 bolts were installed), as shown in Table 2. The zone of class 3 between chainage 10950 and 11200 m required at least 60 bolts, confirming the tunnel face instabilities and the need for additional face bolts in this area. The fault zone necessitated 37 bolts according to the calculations, which is close to the installed value of 30. This zone also included Forepoling installed every 1-2 m, which is not accounted for in the proposed method. In some fault areas, fiberglass dowels were replaced by steel bars to enhance shear strength at the bolt-rock interface.

Table 2 Face reinforcement for different sections of SMP4-3B

Chainage (m)	**11320-11350**	**10950-11200**	**10630-10800**
In-situ stress P_0 (MPa)	15	15	15
Rock mass class	2	3	5
Stability number N	7.9	10.6	23
Tunnel radius r_0 (m)	6.05	6.05	3.15
Total Excavated section $S_t = \pi r_0^2$ (m^2)	115	115	31
Excavated section of Phase A (m^2)	93	93	27
Minimum effective bolt length L' (m)	6	6	6

Installed number of bolts for top heading	50	50	30
Max radial displacement u_m (mm)	193	311	870
Max plastic radius r_{pm} (m)	12.1	14.6	16.1
Tunnel face radial displacement u_0 (mm)	48	72	135
Tunnel face plastic radius r_{p0} (m)	6.6	7.6	6.6
Plastic volume weight F_{vp} (kN)	10 690	16 765	11 041
Corresponding pressure F_{vp} / S_t (kPa)	90	150	360
Bolt supporting force F_b (kN)	257	229	260
Required bolt density (F_{vp} / F_b)/ πr_0^2	0.36	0.635	1.35
Required number of bolts for top heading	34	60	37

5 Conclusions and perspectives

A new simplified analytical method is presented for assessing face reinforcement in deep tunnels within a homogeneous isotropic rock mass, excluding groundwater effects. This method employs the convergence-confinement approach to determine the plastic radius at the tunnel face, which is then used to estimate the plastic volume ahead of the tunnel face. The face reinforcement pattern is incorporated to calculate the supporting bolt pressure. An application of this method is demonstrated in the TELT project, where a tunnel is excavated in squeezing ground conditions, posing challenges to tunnel face stability. The method shows good agreement with the reinforcement scheme implemented in the project. The method can be extended to account for the support installed behind the tunnel face, which directly impacts the extent of the plastic zone ahead of the tunnel face. This face stability approach will be tested on the TELT CO7 works currently being excavated in the squeezing zone at Saint-Martin-la-Porte.

6 Acknowledgments

We are grateful to TELT, the project owner responsible for the works discussed in this communication and the S2IP consortium, the project manager of the site.

7 References

Anagnostou, G, and K Kovári. (1994). The face stability of slurry-shield-driven tunnels. Tunnelling and Underground Space Technology: 165-174.

Anagnostou, G., and P. Perazzelli. (2015). Analysis method and design charts for bolt reinforcement of the tunnel face in cohesive-frictional soils. Tunnelling and Underground Space Technology (47) 162-181.

Broms, B. B., and H. Bennemark. (1967). Stability of clay at vertical openings. Journal of the Soil Mechanics and Foundations Division, ASCE (93): 71-94.

Cantieni, L., G. Anagnostou, and R. Hug. (2011). Interpretation of Core Extrusion Measurements When Tunnelling Through Squeezing Ground. Rock Mech Rock Eng (44): 641-670.

Fernández, F., J. E. Rojas, E. A. Vargas Jr, R. Q. Velloso, and D. Dias. (2021). Three-dimensional face stability analysis of shallow tunnels using Numerical Limit Analysis and Material Point Method. Tunnelling and Underground Space Technology.

Georgiou, D., M. Kavvadas, and A. Kalos. (2021). Numerical investigation of the stability of tunnel excavation faces in deep tunnels. Rockscience International Conference.

Hoek, E. 2023. Tunnels in weak rock. In Practical Rock Engineering.

Janin, JP., T. Rossi, A. Silvestre, F. Laigle, and S. Lione. (2022). Back-analysis on Saint Martin la Porte works of Lyon-Turin base tunnel. ITA-AITES World Tunnel Congress, WTC2022 and 47th General Assembly. Copenhagen. 22-28.

Lunardi, P. (2008). Design and construction of tunnels: Analysis of Controlled Deformations in Rock and Soils (ADECO-RS). Springer Science & Business Media.

Mathieu, E., F. Martin, S. Festa, and S. Pelizza. (2023). New Lyon-Turin Transalpine Rail Link – SMP4 Worksite: A successful experimental crossing of the productive coal deposit. TUNNELS ET ESPACE SOUTERRAIN - N° 286 - Octobre/Novembre/Décembre.

Panet, M., and J. Sulem. 2021. Le calcul des tunnels par la méthode convergence-confinement. Presses de l'École Nationale des Ponts et Chaussées.

Vlachopoulos, N., and M. S. Diederichs. (2009). Improved Longitudinal Displacement Profiles for Convergence Confinement Analysis of Deep Tunnels. Rock Mechanics and Rock Engineering (42): 131-146.